applied sciences

MDPI

Article

Enhancing Performance and Sustainability of Engine Lubricants and Biolubricants by Dispersing SiO_2 Nanoparticles Coated with KH570-Silane Coupling Agent

Homeyra Piri [1], Massimiliano Renzi [1] and Marco Bietresato [1,2,*]

[1] Faculty of Engineering, Free University of Bozen-Bolzano, I-39100 Bolzano, Italy; homeyra.piri@student.unibz.it (H.P.); massimiliano.renzi@unibz.it (M.R.)
[2] Department of Agricultural, Food, Environmental and Animal Sciences (DI4A), University of Udine, I-33100 Udine, Italy
* Correspondence: marco.bietresato@uniud.it; Tel.: +39-0432-558-654

Abstract: One of the technical possibilities to enhance the properties of lubricants and biolubricants is dispersing nanoparticles in them. Although conceptually simple, this operation faces challenges related to: (1) obtaining an initial good dispersion of the nanoparticles in the liquid and (2) ensuring the stability of this dispersion to avoid coalescence. The objective of this study is to verify possible improvements of the stability and characteristics of conventional and bio-based lubricants by efficiently dispersing in them surface-modified SiO_2 nanoparticles. The silane coupling agent KH570 was utilized to modify the surface properties of SiO_2 nanoparticles, facilitating their dispersion within the lubricants. Nanolubricants and nanobiolubricants were prepared using a two-step technique. The dispersion stability of these lubricants was assessed using sedimentation photography, FTIR, and UV-Vis spectrophotometric analyses. The addition of SiO_2 nanoparticles resulted in enhanced physicochemical properties of the resulting lubricant, including slight increases in density and viscosity, as well as a higher viscosity index. Chemical analyses, such as TAN and TBN measurements, confirmed that the nanoparticle addition at various concentrations (0.25%, 0.5%, 0.75%, and 1.0%) did not introduce critical acidity levels or compromise the alkaline reserve. ICP-OES analysis indicated minimal impact on essential additive concentrations, supporting the feasibility of SiO_2 nanoparticles in enhancing lubricant properties without destabilizing additives. The stability of the nanolubricants was monitored over 77 days, with visible sedimentation beginning around the 30th day and becoming more pronounced by the 54th and 77th days. Bio-lubricants exhibited slightly higher sedimentation than conventional lubricants. Optimizing the sonication time proved to be crucial, with longer sonication times (2.5 h) significantly improving the stability of nanolubricants across various concentrations of added nanoparticles. FTIR analysis confirmed the presence of SiO_2 and KH570, indicating no alteration to the basic functional structures of the lubricants and biolubricants. UV-Vis spectrophotometry further underscored the importance of optimizing sonication time for enhanced stability. Overall, this study demonstrates that incorporating surface-modified SiO_2 nanoparticles enhances the properties and stability of conventional and biolubricants, offering potential for improved performance in industrial and engine applications.

Keywords: nano-additives; nanolubricants; nanobiolubricants; nanoparticles dispersion; nanoparticles sedimentation; UV-Vis analysis; stability of lubricants; internal combustion engines

Citation: Piri, H.; Renzi, M.; Bietresato, M. Enhancing Performance and Sustainability of Engine Lubricants and Biolubricants by Dispersing SiO_2 Nanoparticles Coated with KH570-Silane Coupling Agent. *Appl. Sci.* **2024**, *14*, 7943. https://doi.org/10.3390/app14177943

Academic Editor: Mark J. Jackson

Received: 22 July 2024
Revised: 21 August 2024
Accepted: 29 August 2024
Published: 5 September 2024

1. Introduction

In industry and manufacturing, lubricants are essential for maintaining machinery, reducing wear and metal oxidation, and controlling friction and heat in mechanical and electro-mechanical systems [1]. There is a widespread use of lubricants, in particular within agricultural machines and cogeneration units. Indeed, in agricultural machinery, lubricants constitute one of the most important ways to dissipate heat produced from friction and

fuel combustion, but they are also used to operate many types of farm implements, thanks to temporary connections realized through hoses [2,3]. According to the cited references, "a 4WD tractor with a rated engine power of 100 kW requires a total amount of lubricant oil greater than 100 L (about 15 L for the engine, 80 L for the transmission and the hydraulic system, and 10 L for the front and rear axles and the steering system)". Typically, the engine oil is changed at intervals of 500 to 600 h of effective machine operation (or annually), and the transmission oil is changed at intervals of 1200 to 1500 h, resulting in multiple oil changes per year depending on usage. Manufacturers' recommended oil-change intervals must be carefully observed, and crankcases must be refilled when necessary [4]. However, engine overheating, engine oil pressure losses, increased noise, slow start, rapid oil evaporation, oil sludge increase, and oil leakage are the most frequent issues of engine vulnerability in agricultural machines when using engine lubricants of inappropriate quality or not adhering to prescribed oil changes [5]. The above-listed problems may have a major effect on the machinery's longevity and efficiency.

The significance of the lubricant market can be understood by looking at the Italian tractor pool, which had almost 2 million operational units in 2012, as results from the survey made by Federunacoma and reported in [6], with a substantially constant average registration number of 19,430 new units every year since 2012 up to 2023 [7]. This illustrates that the industry of agricultural machines alone represents an enormous market for lubricants. Additionally, in cogeneration units, if looking at a time scale, engine lubricants have to be substituted even more frequently than lubricants used in farm tractors because of the higher number of operating hours per year. In addition, the use of biogas (specifically biomethane) or other alternative clean fuels causes accelerated degradation of lubricant properties, thus constituting one of the most important cost voices in operating biogas plants. To perform machinery maintenance and maintain high energy efficiency, it is therefore essential to improve properties of lubricants such as viscosity, thermal stability, and oxidation resistance. Today, different lubricants are designed for a range of different mechanical applications (e.g., high-load industrial gearboxes, high-speed spindles, and automotive engines), highlighting their value in machinery and equipment in general [8]. Mineral-based or synthetic lubricants frequently do not meet the requirements of the equipment makers. In order to improve qualities like anti-oxidation, tribology, and thermal performance, additives (e.g., antioxidants, anti-wear agents, and viscosity index improvers) are introduced into the base oil formulation to address this problem [9]. By enhancing their physical and chemical properties, these additives are essential in lowering friction and, consequently, wear in machinery [10]. Nanomaterials possess particular chemical and physical features, and they are distinguished by their overall sizes, shapes, and surface effects [11]. According to certain studies, when only a small amount of spherical, pseudo-spherical, or amorphous nanoparticles is used as a lubricant additive, hence composing a so-called "nanolubricant", it is possible to significantly improve the performance of the base lubricating oil [12], resulting in significant advantages such as friction reduction, anti-wear properties, remarkable self-healing capabilities, reduced energy consumption, and enhanced environmental protection [11,13].

Researchers have been concentrating on nanolubricants for a variety of reasons, such as their capability to lower friction and wear, but particle suspension is the primary challenge to the creation of novel nanolubricants [14]. Preventing nanoparticle aggregation is essential for efficiently improving lubrication in a contact area and granting a uniformity of action of these lubricants from the beginning to the end of their use [15]. For the development of innovative lubricants and their formulation, the achievement of dispersion principles is fundamental [14]. To achieve optimal dispersion, a variety of chemical–physical processes, including ultrasonication, homogenization, and particle surface modification, is applied [16]. The good dispersion of nanolubricants can be probed using a variety of methods, each of which provides a different perspective regarding the way they function. Some of these techniques include:

1. Visual Inspection: the dispersion is directly inspected visually in order to detect any observable (macro-)accumulation or deposition of nanoparticles [17–21].
2. Dynamic light scattering (DLS): by measuring the hydrodynamic radius of nanoparticles, it is possible to discern the occurrence of accumulation [22].
3. UV-visible spectroscopy (UV-Vis): by analysing light absorption patterns, it is feasible to discover the tendency of nanoparticles to accumulate and precipitate [20,21,23,24].
4. Zeta Potential: the dispersion stability of nanolubricants is measured via zeta potential (electric potential at the slipping plane) analysis, where higher zeta potential values (positive or negative) indicate better stability [16].
5. Fourier Transform Infrared Spectroscopy (FTIR): this technique is used to indicate stable physical interactions between the dispersed nanoparticle and the base lubricant oil, providing insights into chemical compatibility and bonding [25].

Mohd Farid Ismail et al. [26] evaluated the stability of TiO_2 and SiO_2 nanoparticles in Polyvinyl ether (PVE) lubricant using visual observation, UV-Vis spectrophotometric analysis, and zeta potential measurements. The concentration ratio of the TiO_2/PVE nanolubricant remained at 95% for a duration of 30 days during the study. After 7 h of sonication, the TiO_2/PVE, SiO_2/PVE, and SiO_2-TiO_2/PVE samples showed zeta potential values of 203.1 mV, 224.2 mV, and 105.3 mV, respectively. Sharif et al. [21] employed sedimentation photography and UV-Vis spectrophotometry to evaluate the stability of SiO_2/Polyalkylene Glycol (PAG) nanolubricant. The results indicated a low level of sedimentation seen throughout a one-month timeframe. The UV-Vis test provided additional confirmation of the stability of the studied nanolubricant, as it maintained a relative concentration for nanoparticles of over 70% compared to its initial concentration. Gulzar et al. [20] showed that nano-TiO_2/SiO_2 exhibited significant dispersion properties, particularly at a concentration of 0.75 wt%, even in the absence of a surfactant. The homogenous dispersion of the substance not only led to a stable suspension, but also demonstrated its effectiveness in reducing friction and wear, as compared to a blank palm trimethylolpropane (TMP) ester. The rheological behaviour and tribological characteristics of a nano-lubricant comprising SiO_2 nanoparticles in an SAE40 engine oil were studied by Kashefi et al. According to their research, adding SiO_2 nanoparticles significantly improved a number of important features. At a 0.1% nanoparticle concentration, the study saw a 50% reduction in wear rate and an 18.46% decrease in the friction coefficient. Furthermore, the lubricant's flash point increased by 3.8% as a result of the nanoparticle addition [27]. However, enhancing the stability of nanolubricants requires a comprehensive strategy that extends beyond simple physical treatments. Integrating chemical techniques with physical methods, such as adding surfactants and modifying the surface properties of nanoparticles, results in a nanolubricant formulation that is more resistant to corrosion. This improved resistance pertains to both protecting the material surfaces in contact with the nanolubricant and ensuring the chemical stability of the nanoparticles themselves.

The widespread consumption of petroleum-based lubricants has given rise to growing concerns, sparking an increasing interest in the use of readily biodegradable alternatives, particularly biolubricants [28]. In addition to this fact, there is also the inevitable leakage of lubricants on the ground that occurs in fast connectors for hoses used to connect agricultural tractors and implements, as well as used in construction machinery to connect different attachments. According to an informal survey conducted among contractors in Northwest Italy, it was found that hydraulic couplers without oil collectors can result in oil leaks of up to 2 L per year per tractor [29,30]. Biolubricants, including plant oils, animal fats, or their chemically modified derivatives, are generally acknowledged for their environmentally friendly characteristics due to their exceptional biodegradability and renewable feedstock [31]; in addition, they constitute the ideal evolution of currently used synthetic and mineral lubricants.

So, the idea behind the experimentation illustrated in this article is to propose and test the properties of a mix of nanoparticles and biolubricant, namely a "nano-bio-lubricant". This novel lubricant showed the enhanced properties of all nanolubricants, which were well

described in the literature, together with better biodegradability/environmental compatibility of biolubricants, in a formulation that bridged actual and future mechanical systems.

Therefore, this article assessed the importance of silicon dioxide (SiO_2) nanoparticles coated with a KH570-Silane coupling agent, concentrating on their use in conventional and eco-friendly biolubricants. Specifically, SiO_2 was selected for its advantageous additive effects, such as its ability to efficiently minimize wear and friction of components in relative motion, in addition to its biocompatibility, which is crucial for applications involving environmental and health concerns. Indeed, SiNPs, specifically SiO_2 nanoparticles, have been extensively studied and are widely used in biomedical applications, where safety is of utmost concern. For example, the study by Maria Ada Malvindi et al. [32] demonstrates that SiO_2 nanoparticles exhibit high biocompatibility across various cell lines, with no significant cytotoxic effects observed under specific conditions. Instead, γ-methacryloyloxypropyltrimethoxysilane, or KH570, was selected for surface modification applications because of its known efficacy. It interacts with the surface hydroxyl groups of silicon dioxide nanoparticles through the presence of a hydrolyzable ethoxy group. Furthermore, KH570's amino group offers functional groups for additional reactions or attachments to other substances or molecules. By modifying the surface of SiO_2 nanoparticles, the KH570-Silane coupling agent improves their compatibility with diverse systems and increases their dispersibility in a range of matrices or solvents. By strengthening their surface modification, SiO_2 nanoparticles become more stable, which decreases aggregation and boosts their overall performance across a range of applications. Specifically, the study evaluates the stability of SiO_2 nanoparticles in Mistral 15W40 lubricant, by NILS S.p.A (Postal, Bolzano, Italy), and PLANTO MOT SAE 10W40 biolubricant, by FUCHS LUBRICANTS GERMANY GmbH (Mannheim, Germany), over a set reference period (77 days), which is sufficient to allow evaluation of any early onset sedimentation in the samples. It investigates and assesses the stability of four varied nanoparticle concentrations. Visual evaluations, FTIR, and UV-Vis spectrometer absorbance measurements are employed in the analysis to determine the stability of nanolubricants. The intention of this comprehensive investigation is to ascertain how effectively the KH570-Silane coupling agent preserves nanoparticle stability and dispersion in conventional and biolubricant systems. A thorough analysis of the physicochemical characteristics of nanolubricants and nanobiolubricants is additionally included in the study. The purpose of this investigation is to: (1) develop high-performance lubricants that exceed industry requirements and guarantee the dependability and effectiveness of diverse mechanical and industrial applications through the process of these exhaustive investigations; (2) propose a protocol for preparing the nanolubricants and nanobiolubricants and verify its effectiveness in terms of stability and improvement of the characteristics of the resulting products.

2. Materials and Methods

2.1. Materials

Silicon dioxide (SiO_2) nanoparticles were coated with the KH570-Silane coupling agent; both these materials were obtained from Nanografi Inc. (Çankaya/Ankara, Turkey; https://nanografi.com/). The properties of the nanoparticles together with some data coming from an elemental analysis of nanoparticles coated with the above-indicated coupling agent are shown in Tables 1 and 2, respectively. The molecular structure of the silane-coupling agents (3-Methacryloxypropyltrimethoxy silane) is presented in Figure 1 and the chemical formula of KH570 is $CH_3CCH_2COO(CH_2)_3Si(OCH_3)_3$ [33]. It has a molecular mass equal to 248.351 $g \cdot mol^{-1}$. The designation given to this particular silane coupling agent is shorter than IUPAC designation because it is only a reference within producers' product lines, so letters (KH) and numbers (570) do not have any specific meaning beyond serving as an identifier for this product. Mistral 15W40 lubricant and PLANTO MOT SAE 10W40 biolubricant were supplied from NILS S.p.A (https://www.nils.eu/) and FUCHS LUBRICANTS GERMANY GmbH (https://www.fuchs.com/de/en/), respectively. In Table 3, the technical characteristics of the lubricant and biolubricant are presented separately. The scientific methods utilized

in this research include: viscometric analysis, FTIR spectroscopy, UV-Vis spectrophotometry, and ICP-OES analysis. The standards referenced in the measurements are provided by the American Society for Testing and Materials (ASTM) International (https://www.astm.org/) and the International Organization for Standardization (ISO; https://www.iso.org/). The techniques encompass a two-step preparation of nanolubricants and nanobiolubricants, magnetic stirring, ultrasonic cleaning, and sedimentation photography. The employed analyses are: kinematic viscosity measurements, viscosity index calculation, density measurement, TAN and TBN titration, and elemental analysis. The software used includes the instrument-specific software for the Anton Paar SVM 3001 kinematic viscometer (Anton Paar GmbH, Graz, Austria; https://www.anton-paar.com/), the Mettler Toledo T50 titrator (Mettler-Toledo International Inc., Columbus, OH, USA; https://www.mt.com/), the Perkin Elmer OPTIMA 8000 ICP-OES (PerkinElmer Inc., Waltham, MA, USA; https://content.perkinelmer.com/), the Perkin Elmer Spectrum 100 FTIR (PerkinElmer Inc., Waltham, MA, USA; https://content.perkinelmer.com/), and the Agilent Cary 100 UV-Visible Spectrophotometer (Agilent Technologies Inc., Santa Clara, CA, USA; https://www.agilent.com/). All research activities were conducted in the university laboratory of the Free University of Bozen-Bolzano.

Table 1. SiO_2 nanoparticles properties.

Technical Property	Unit of Measurement	Value
Purity	%	95.9+
Colour	–	white
Particle shape	–	amorphous
Average Particle Size	nm	18–35
Specific Surface Area	$m^2 \cdot g^{-1}$	150–550
Bulk Density	$g \cdot cm^{-3}$	<0.1
True Density	$g \cdot cm^{-3}$	2.2

Table 2. Elemental Analysis of nanoparticles coated with KH570-Silane coupling agent.

Element	wt%
SiO_2	95.9
KH570	3–4
Fe	0.032
Ca	0.056
Mg	0.0085
S	0.025

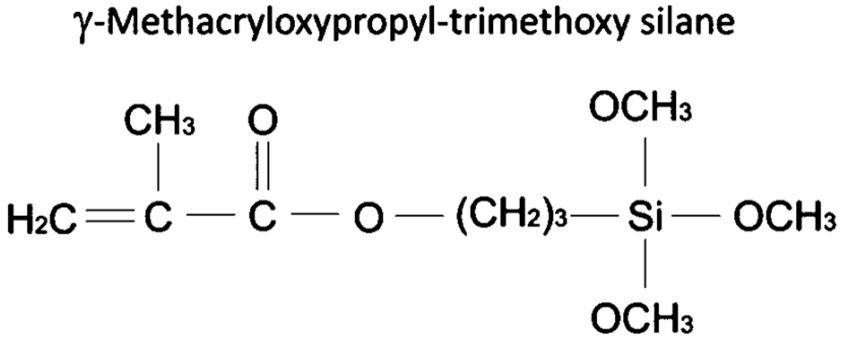

Figure 1. Molecular structure of the KH570 silane coupling agent [34].

Table 3. Technical characteristics of lubricant (Mistral 15W40) and biolubricant (PLANTO MOT SAE 10W40).

Property	Unit of Measurement	Reference	Mistral 15W40	PLANTO MOT SAE 10W40
Kinematic viscosity at 40 °C	cSt	ASTM D445-24 [35]	97.3	87.0
Kinematic viscosity at 100 °C	cSt	ASTM D445-24 [35]	13.5	13.7
Viscosity index	–	ISO 2909:2002 [36]	138	160
Density at 15 °C	$g \cdot cm^{-3}$	ASTM D4052-22 [37]	0.8769	0.8719
TBN	$mg(KOH) \cdot g^{-1}$	ASTM D4739-17 [38]	10.5	9.7
TAN	$mg(KOH) \cdot g^{-1}$	ASTM D664-18e2 [39]	2.2	1.7

2.2. Formulation of Nanolubricants and Nanobiolubricants

The nanolubricants/nanobiolubricants used in this study were formulated utilizing a two-step technique shown in Figure 2. The nanoparticles were dispersed in both lubricant and biolubricant samples at various concentrations to provide the corresponding nanolubricants, including 0.25, 0.50, 0.75, and 1.00 wt%. In order to achieve optimal stability and uniformity, the samples underwent magnetic stirring for 1.5 h at a speed of 1500 rpm. Subsequently, the samples were subjected to the action of an ultrasonic Cleaner VWR USC600THD (VWR International, Radnor, PA, USA; https://www.vwr.com/) that utilizes ultrasound waves at a frequency of 45 kHz and with a power output of 120 W for a period of 2.5 h. The specifications of the nanolubricants and nanobiolubricants are shown in Table 4.

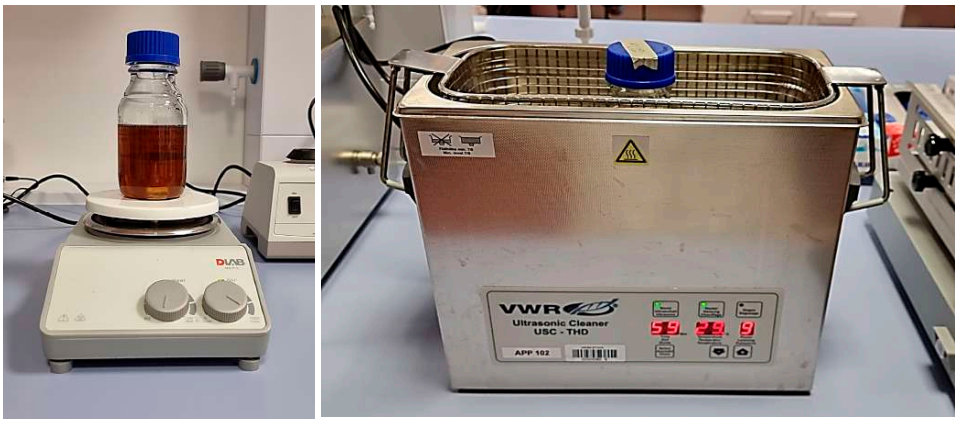

Figure 2. Two-step preparation technique for nanolubricants.

Table 4. Composition and Specifications of Nanolubricants and nanobiolubricants.

Sample Number	SiO_2 (wt%)	Stirring Time (h)	Sonication Time (h)
1.1	0.25	1.5	0.0
1.2	0.25	1.5	1.0
1.3	0.25	1.5	2.5
2.1	0.50	1.5	0.0
2.2	0.50	1.5	1.0
2.3	0.50	1.5	2.5
3.1	0.75	1.5	0.0
3.2	0.75	1.5	1.0
3.3	0.75	1.5	2.5
4.1	1.00	1.5	0.0
4.2	1.00	1.5	1.0
4.3	1.00	1.5	2.5

2.3. Physicochemical Properties of Nanolubricants and Nanobiolubricants

In this study, viscometric analysis was employed to evaluate the critical attributes of nanolubricants and nanobiolubricants. Kinematic viscosity was measured at both 40 °C and 100 °C to determine the resistance of the lubricants to flow under gravitational forces. These measurements are crucial as they directly influence the lubricants' performance in reducing friction and wear in mechanical systems [40]. Additionally, the viscosity index was calculated to understand the changes in viscosity with temperature variations, which is essential for predicting lubricant behaviour under different operating conditions [41]. The density at 15 °C, representing the mass per unit volume, was also measured to provide insights into the formulation and stability of the lubricants. These assessments were conducted using an Anton Paar SVM 3001 kinematic viscometer, known for its high precision with a density accuracy of 0.0001 $g \cdot cm^{-3}$ and a viscosity accuracy of 0.001 $mm^2 \cdot s^{-1}$. Conducting these tests is vital for developing high-performance lubricants that meet industry standards and ensure the reliability and efficiency of various mechanical and industrial applications.

Total Acid Number (TAN) and Total Base Number (TBN) are critical indicators of the chemical stability and neutralization capacity of lubricants. The TAN measures the acidity, indicating the presence of acidic components, while the TBN measures the alkalinity, indicating the lubricant's ability to neutralize acids [42]. The TBN and TAN were determined using a titrator, specifically the Mettler Toledo T50, with a precision of TBN = 0.01 $mg(KOH) \cdot g^{-1}$ and TAN = 0.001 $mg(KOH) \cdot g^{-1}$. Inductively coupled plasma optical emission spectroscopy (ICP-OES) analysis, conducted with a Perkin Elmer OPTIMA 8000 instrument, provides detailed information about the elemental composition of the lubricants. This includes quantification of metal concentrations, such as wear elements like Fe and Cr, pollution elements, and additive elements, with a precision of 1 ppm. These measurements are crucial for assessing equipment wear, lubricant contamination, and additive effectiveness.

2.4. Dispersion Analysis

Different methodologies can be employed to evaluate the stability of nanolubricants, which is intended as the avoidance of any phenomenon concerning nanoparticles and the alteration of their uniformity of distribution in the mass of the liquid hosting them (e.g., precipitation, floating, aggregation). This investigation aimed to assess the comparative stability of the nanosuspension by employing sedimentation photography, FTIR, and UV-Vis spectrophotometry [20,43–45]. Sedimentation photography is an invaluable technique for observing the settling characteristics of nanoparticles in a suspension. The experiment entailed obtaining images of the nanolubricant at precise time intervals subsequent to its preparation. The purpose of these photographs was to observe the sedimentation of SiO_2 nanoparticles that were coated with the KH570-silane coupling agent in the lubricant. The variations in the dispersion quality and settling rate were analysed with time, yielding useful insights into the stability of the nanolubricant. FTIR is another vital tool employed in assessing the stability of nanolubricants. FTIR spectroscopy provides valuable information regarding the chemical composition and structural changes within the nanolubricant. By analysing the infrared absorption spectra of the nanolubricant, any alterations in molecular bonds or functional groups can be detected. These changes can be indicative of interactions between the nanoparticles and the lubricant matrix [25,46]. The instrument used for FTIR analysis was a Perkin Elmer Spectrum 100, enabling precise measurements of infrared spectra. UV-Vis spectrophotometry is a precise method used to measure the concentration and dispersion of nanoparticles in a liquid media. Due to the high viscosity of the used lubricants, they were first diluted with a ratio of 1:10 using hexane as the solvent to facilitate the UV analysis. The nanolubricants' absorption spectra were measured at specified wavelengths, which were determined through a comprehensive scanning process. This approach ensured precise determination of nanoparticle concentration and distribution within the lubricant. Fluctuations in the absorbance spectrum could indicate changes in the dispersion of nanoparticles, which, in turn, affects the stability of the nanolubricants [47,48]. The instrument used was an Agilent Cary 100 UV-Visible Spectrophotometer, as shown in Figure 3.

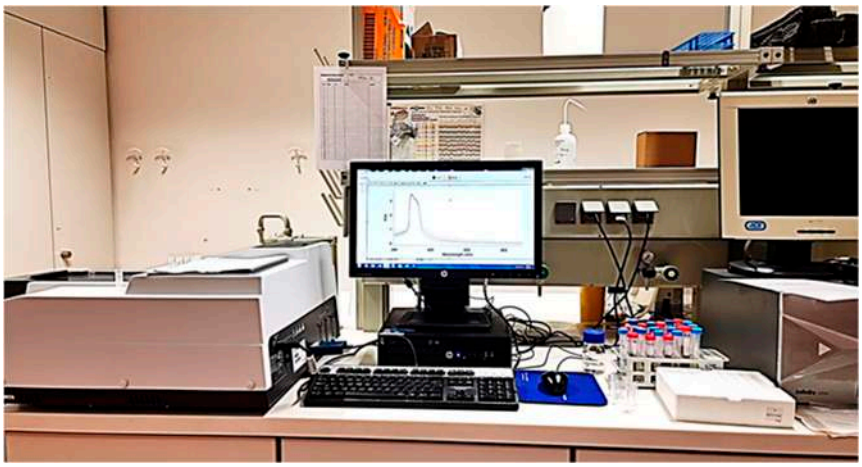

Figure 3. Agilent Cary 100 UV-Visible Spectrophotometer.

3. Results and Discussion

3.1. Characterization and Assessment of Nanolubricants and Nanobiolubricants

The kinematic viscosity at 40 °C and 100 °C, the density at 15 °C, and the viscosity index of all samples, including pure lubricants/biolubricants and nanolubricants/nanobiolubricants, are comprehensively measured and presented in Tables 5 and 6 for comparison and analysis. These measurements provide critical insights into the performance characteristics of each lubricant type under various conditions. Both nanolubricants and nanobiolubricants exhibit a consistent dark yellow appearance and a characteristic smell across all samples, indicating no significant changes in these sensory properties with the addition of SiO_2 nanoparticles. For nanolubricants, the density increases slightly with higher concentrations of SiO_2, from 0.8769 g·cm^{-3} for pure lubricant to 0.8842 g·cm^{-3} for 1.00% SiO_2 nanolubricant. Similarly, nanobiolubricants show a gradual increase in density from 0.8719 g·cm^{-3} for pure biolubricant to 0.8770 g·cm^{-3} for 1.00% SiO_2 nanobiolubricants. The increase in density suggests that the incorporation of SiO_2 nanoparticles results in a denser formulation due to the addition of solid particles. The viscosity at 40 °C and 100 °C show a slight increase with higher SiO_2 content for both nanolubricants and nanobiolubricants. For nanolubricants, the viscosity at 40 °C ranges from 97.3 cSt (pure) to 99.9 cSt (1.00% SiO_2), and at 100 °C from 13.5 cSt (pure) to 14.0 cSt (1.00% SiO_2). For nanobiolubricants, the viscosity at 40 °C ranges from 87.0 cSt (pure) to 90.3 cSt (1.00% SiO_2), and at 100 °C from 13.7 cSt (pure) to 14.4 cSt (1.00% SiO_2). The slight increase in viscosity indicates improved resistance to flow, which can enhance lubrication properties and reduce wear [40,49,50]. The viscosity index shows improvement with increasing SiO_2 content for both types of lubricants. Nanolubricants' viscosity index rises from 138 (pure) to 143 (1.00% SiO_2). Nanobiolubricants' viscosity index increases more significantly, from 160 (pure) to 166 (1.00% SiO_2). A higher viscosity index indicates better stability of the lubricant's viscosity across temperature changes, which is beneficial for maintaining performance under varying operating conditions [51].

The TAN values for all samples, including the base lubricants (Mistral 15W40 and PLANTO MOT SAE 10W40) and nanolubricants, are below 3.0 mg(KOH)·g^{-1}. This is generally considered acceptable for lubricants. The slight variations among the samples are not significant enough to cause concern, indicating that the addition of SiO_2 nanoparticles does not significantly increase acidity and might even help in stabilizing it. However, as the concentration of SiO_2 increases, there is a gradual increase in acidity. While these values are not immediately critical, the trend suggests that higher concentrations of SiO_2 could lead to higher acidity over time. The TBN values remain stable and high, around 10.3 to 10.7 mg(KOH)·g^{-1}, across all samples of nanolubricants and around 9.5 to 9.9 mg(KOH)·g^{-1} for nanobiolubricants. This indicates that the nanolubricants have a strong capacity for neutralizing acids, and the addition of SiO_2 nanoparticles does not adversely affect the alkaline reserve of the lubricants.

This stability suggests that the nanolubricants, despite having a slightly higher acidity, could potentially offer enhanced corrosion resistance, as suggested by recent research on the use of metal and oxide nanoparticles [52,53]. However, specific corrosion tests would be required to confirm their effectiveness in protecting against corrosion.

Table 5. Physicochemical Properties of Nanolubricants.

Property	Lubricant (Pure) Mistral 15W40	Nanolubricants 0.25% SiO_2	Nanolubricants 0.50% SiO_2	Nanolubricants 0.75% SiO_2	Nanolubricants 1.00% SiO_2
Appearance	dark yellow	dark yellow	dark yellow	dark yellow	dark yellow
Smell	characteristic	characteristic	characteristic	characteristic	characteristic
Density at 15 °C [g·cm^{-3}]	0.8769	0.8808	0.8819	0.8831	0.8842
Viscosity at 40 °C [cSt]	97.3	97.6	98.4	99.0	99.9
Viscosity at 100 °C [cSt]	13.5	13.7	13.8	13.9	14.0
Viscosity Index [–]	138	141	142	142	143
TAN [mg(KOH)·g^{-1}]	2.17	1.9	1.9	2.1	2.2
TBN [mg(KOH)·g^{-1}]	10.6	10.7	10.3	10.3	10.3
Pollution–silicon [ppm]	65	419	738	1101	1365
Pollution–sodium [ppm]	0	0	0	0	2
Additives–calcium [ppm]	3045	3118	3124	3084	3043
Additives–magnesium [ppm]	71	71	72	74	70
Additives–zinc [ppm]	928	926	923	915	889
Additives–phosphorus [ppm]	766	827	798	809	795
Additives–boron [ppm]	137	131	131	130	126
Additives–molybdenum [ppm]	6	9	9	9	9

Table 6. Physicochemical Properties of Nanobiolubricants.

Property	Biolubricant (Pure) SAE 10W40	Nanobiolubricants 0.25% SiO_2	Nanobiolubricants 0.50% SiO_2	Nanobiolubricants 0.75% SiO_2	Nanobiolubricants 1.00% SiO_2
Appearance	dark yellow	dark yellow	dark yellow	dark yellow	dark yellow
Smell	characteristic	characteristic	characteristic	characteristic	characteristic
Density at 15 °C [g·cm^{-3}]	0.8719	0.8733	0.8746	0.8758	0.877
Viscosity at 40 °C [cSt]	87.0	87.9	88.6	89.6	90.3
Viscosity at 100 °C [cSt]	13.7	14	14.2	14.3	14.4
Viscosity Index [–]	160	164	165	166	166
TAN [mg KOH·g^{-1}]	1.7	2.2	2.4	2.5	2.6
TBN [mg KOH·g^{-1}]	9.7	9.5	9.6	9.9	9.6
Pollution–silicon [ppm]	2	337	702	1020	1402
Pollution–sodium [ppm]	0	0	0	0	5
Additives–calcium [ppm]	1672	1720	1737	1720	1761
Additives–magnesium [ppm]	333	345	353	351	359
Additives–zinc [ppm]	693	690	678	668	658
Additives–phosphorus [ppm]	593	596	594	587	591
Additives–boron [ppm]	487	472	459	462	476
Additives–molybdenum [ppm]	74	73	75	73	74

The ICP-OES analysis reveals distinct trends in elemental concentrations due to the addition of SiO_2 nanoparticles in both nanolubricants and nanobiolubricants. The significant increase in silicon levels correlates with higher concentrations of SiO_2, which is expected and confirms the presence of SiO_2 nanoparticles. This increase is not indicative of contamination but rather reflects the intentional incorporation of SiO_2 nanoparticles, serving as a source of silicon. Sodium levels remain minimal across the samples, with a slight increase observed only at the highest SiO_2 concentration (1.00 wt% SiO_2). This minimal fluctuation indicates that sodium contamination is negligible and does not significantly impact the overall composition of the lubricants.

The analysis of essential additives reveals that the concentrations of calcium, magnesium, and phosphorus remain stable despite the addition of SiO_2 nanoparticles. This stability indicates that the inclusion of SiO_2 does not significantly alter the levels of these critical additives, thereby maintaining the functional integrity of the lubricants. However,

slight decreases are observed in the levels of zinc and boron. While these changes are minor, they should be monitored to ensure that they do not affect the performance of the lubricants over time. Additionally, molybdenum shows a slight increase in nanolubricants, which could potentially enhance certain lubricant properties such as anti-wear performance. Interestingly, in nanobiolubricants, molybdenum levels remain stable, suggesting a differential interaction between the base fluids and the nanoparticles.

3.2. Visual Nanoparticle Settling Assessment

All nanolubricants samples were observed on days 0, 1, 3, 7, 15, 30, 54, and 77 after preparation. Visible changes were not apparent until the 30th day. Figure 4 shows a comparison of both nanolubricants samples up to 77 days after preparation for different sonication times (0 h, 1 h, and 2.5 h). On the first day of observation, all samples appeared to be dispersed well and it was difficult to differentiate them with the naked eye. Starting from the 30th day, a small number of nanoparticles began to deposit in the form of a white layer at the bottom of the cuvettes. This sedimentation gradually increased, becoming more noticeable by the 54th and 77th days. It was observed that the amount of sedimentation in bio-lubricants was slightly higher than in conventional lubricants. However, the effect of different sonication times on the amount of sedimentation was not entirely clear by visual inspection alone. This difference should be measured more accurately using a UV-Vis spectrophotometer.

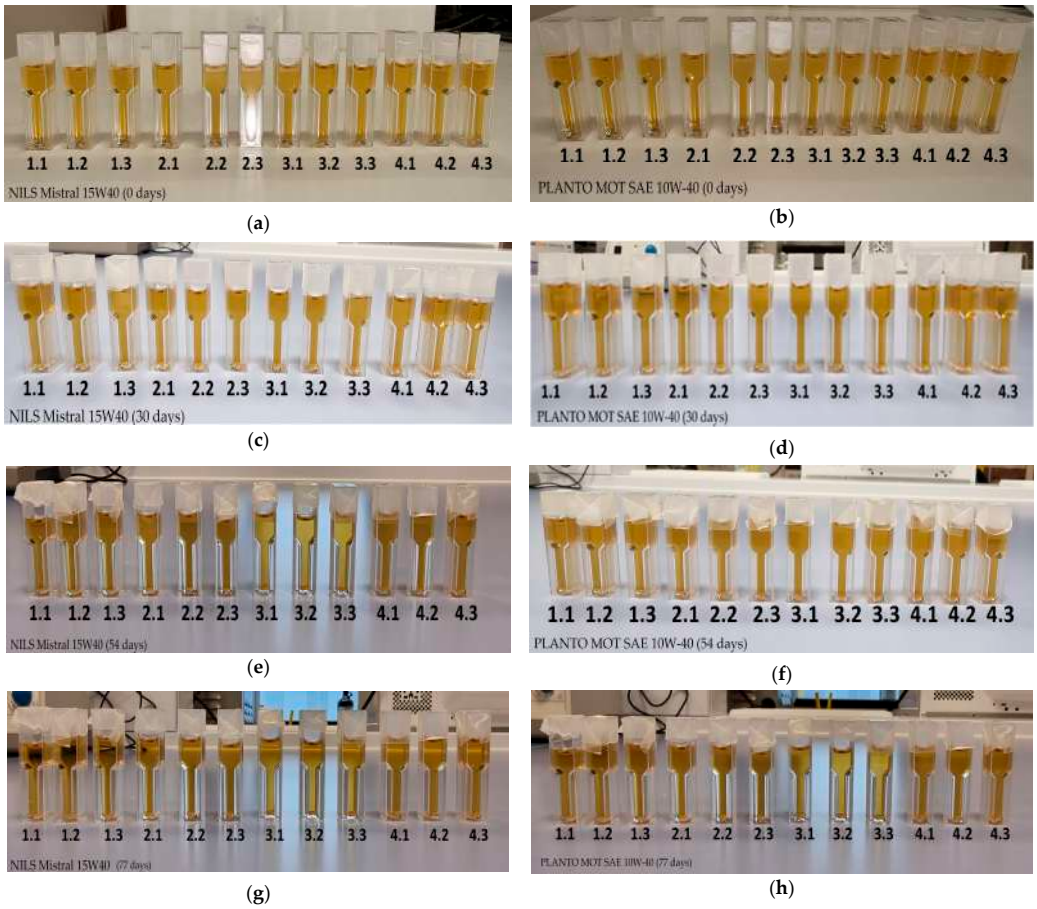

Figure 4. Static stability of nanolubricant samples with different sonication times: (**a**) after preparation (Mistral 15W40); (**b**) after preparation (PLANTO MOT SAE 10W40);(**c**) after 30 days (Mistral 15W40); (**d**) after 30 days (PLANTO MOT SAE 10W40); (**e**) after 54 days (Mistral 15W40); (**f**) after 54 days (PLANTO MOT SAE 10W40); (**g**) after 77 days (Mistral 15W40); (**h**) after 77 days (PLANTO MOT SAE 10W40).

3.3. FTIR Characterization of Nanolubricant Stability

The FTIR spectra for the SiO_2 nanoparticles coated with the KH570 silane coupling agent, the reference lubricant (Mistral 15W40) and its nanolubricants, as well as the reference biolubricant (PLANTO MOT SAE 10W40) and its nanobiolubricants, are presented in the following figures. A detailed comparison of the peaks of both lubricants and biolubricants is shown in Figure 5, and Table 7 compares them in detail. The biolubricant shows strong O-H stretching peaks (3649.1 cm^{-1} and 3458.9 cm^{-1}), indicating the presence of hydroxyl groups, which are typical in natural esters and bio-based additives. Both lubricants exhibit strong C=O stretching peaks, but the biolubricant has a single intense peak (1740.0 cm^{-1}), reflecting its ester-rich formulation. The biolubricant has a notable peak at 1605.6 cm^{-1}, suggesting the presence of unsaturated components (C=C stretching). The biolubricant shows a peak at 1515.9 cm^{-1}, which could derive from certain additives (N-O asymmetric stretching). Both lubricants have CH_2 and CH_3 bending vibrations, but the conventional lubricant has a broader set of hydrocarbon-related peaks. The biolubricant displays peaks indicative of aromatic or unsaturated components, which are less pronounced in the conventional lubricant. These differences reflect the distinct nature of their formulations, as conventional lubricants rely heavily on refined hydrocarbon oils and synthetic additives, while biolubricants incorporate natural esters and bio-based components, thus leading to distinct spectral features [54–56].

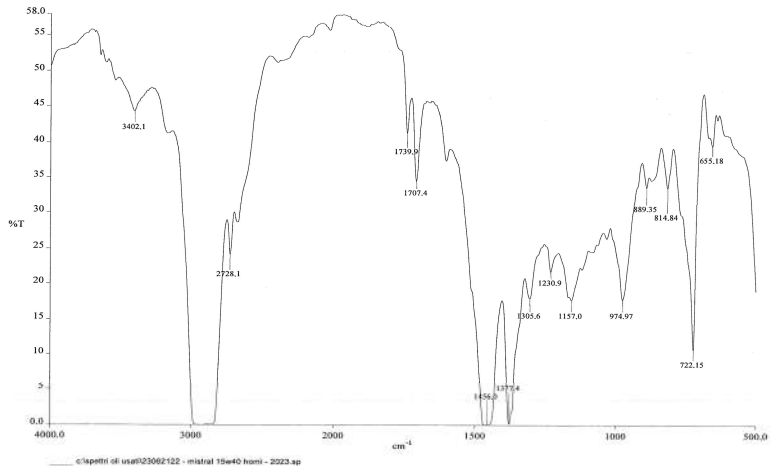

(**a**)

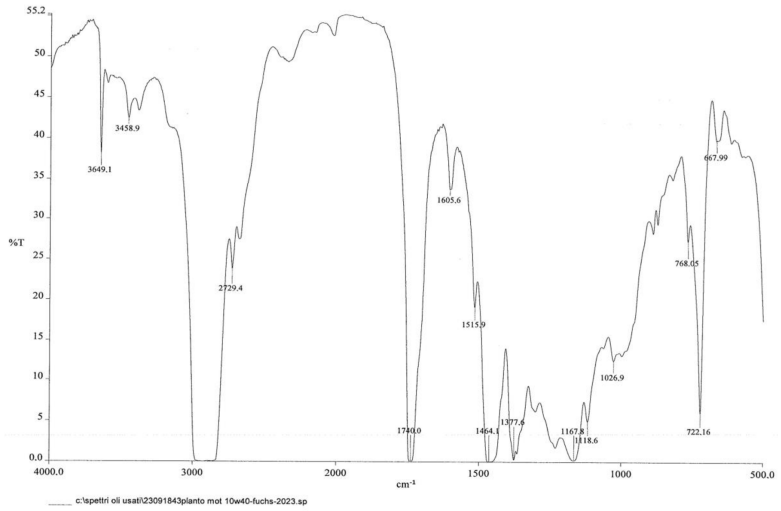

(**b**)

Figure 5. FTIR spectra: (**a**) lubricant (Mistral 15W40), (**b**) biolubricant (PLANTO MOT SAE 10W40).

Table 7. Comparative FTIR Spectral Analysis of Conventional Lubricant (Mistral 15W40) and Biolubricant (PLANTO MOT SAE 10W40).

Wavelength (cm^{-1})	Mistral 15W40	PLANTO MOT SAE 10W40	Interpretation
3649.1	-	Peaks present	O-H stretching (hydroxyl groups)
3458.9	-	Peaks present	O-H stretching (hydroxyl groups)
3402.1	Peaks present	-	O-H stretching (hydroxyl groups)
2729.4	-	Peaks present	C-H stretching (hydrocarbons or additives)
2728.1	Peaks present	-	C-H stretching (hydrocarbons or additives)
1740.0	-	Peaks present	C=O stretching (esters)
1739.9	Peaks present	-	C=O stretching (esters)
1707.4	Peaks present	-	C=O stretching (esters)
1605.6	-	Peaks present	C=C stretching (unsaturated components)
1515.9	-	Peaks present	N-O asymmetric stretching (additives)
1464.4	-	Peaks present	CH_2 bending (hydrocarbon chains)
1456.0	Peaks present	-	CH_2 bending (hydrocarbon chains)
1377.9	-	Peaks present	CH_3 bending (hydrocarbon chains)
1377.4	Peaks present	-	CH_3 bending (hydrocarbon chains)
1305.6	Peaks present	-	C-O stretching (esters)
1230.9	Peaks present	-	C-O stretching (esters)
1167.8	-	Peaks present	C-O stretching (esters)
1157.0	Peaks present	-	C-O stretching (esters)
1118.6	-	Peaks present	C-O stretching (esters)
1026.9	-	Peaks present	C-O stretching (esters)
974.97	Peaks present	-	Various hydrocarbon-related vibrations
889.35	Peaks present	-	Various hydrocarbon-related vibrations
814.84	Peaks present	-	Various hydrocarbon-related vibrations
768.05	-	Peaks present	Aromatic or unsaturated components
722.16	Peaks present	Peaks present	CH_2 rocking (long hydrocarbon chains)
667.99	-	Peaks present	Aromatic or unsaturated components
655.18	Peaks present	-	Aromatic or unsaturated components

Figure 6 highlights several distinct peaks at wavenumbers 1089.69 cm^{-1}, 800 cm^{-1}, 463.66 cm^{-1}, and a smaller peak at 1636 cm^{-1}. These peaks correspond to specific vibrational frequencies of molecular bonds within the samples. The peak at 1089.69 cm^{-1} is characteristic of Si-O-Si asymmetric stretching, the peak at 800 cm^{-1} is attributed to Si-O-Si symmetric bending, the peak at 463.66 cm^{-1} is due to Si–Si–O bending vibrations, and the peak at 1636 cm^{-1} corresponds to the C=O stretching of the ester group in KH570. These findings confirm the presence of both SiO_2 and the KH570 silane coupling agent in the samples [57,58]. To analyse the chemical compositions of the nanolubricants, Figure 7a,b present the FTIR spectra for the reference lubricant (Mistral 15W40) and its nanolubricants at four different concentrations (0.25, 0.50, 0.75, and 1.00 wt%), as well as for the reference biolubricant (PLANTO MOT SAE 10W40) and its nanolubricants at the same concentrations. The absence of chemical by-products in the spectra confirms that no chemical reactions have occurred between the dispersed SiO_2 nanoparticles and the lubricants or biolubricants. These findings demonstrate that the basic functional structures of the lubricants and biolubricants remain unchanged, indicating excellent chemical stability [25,50].

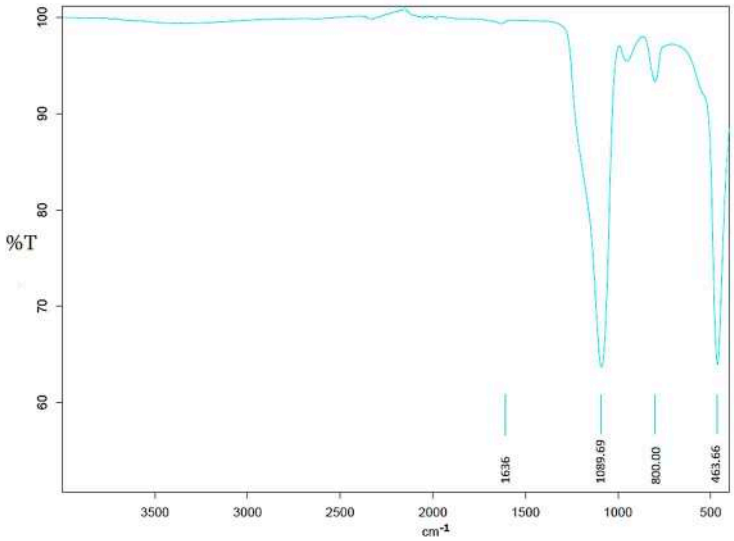

Figure 6. FTIR spectra: SiO_2 nanoparticles coated with KH570-silane coupling agent.

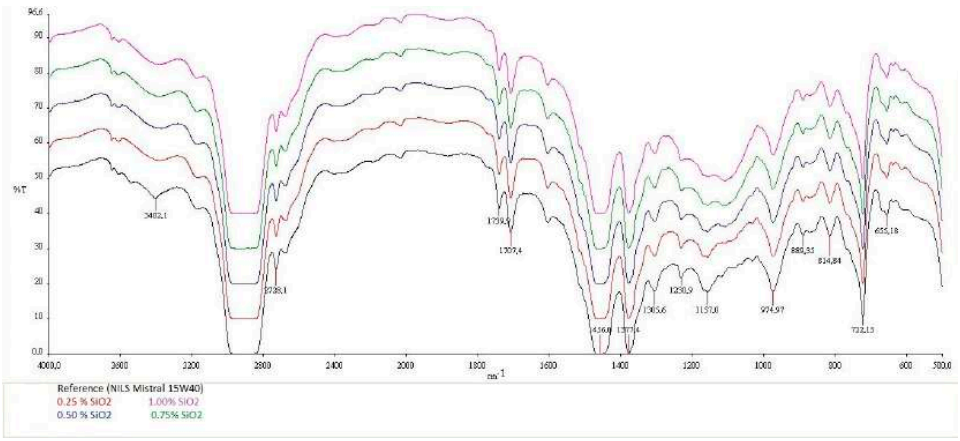

(**a**)

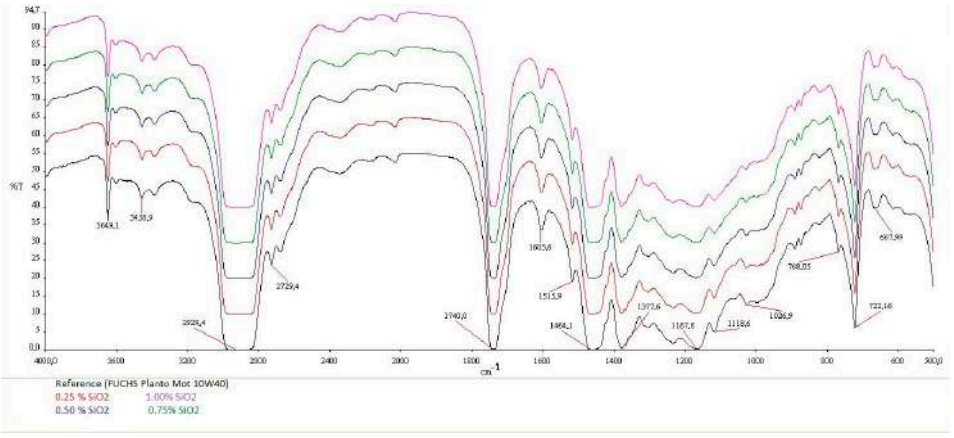

(**b**)

Figure 7. FTIR spectra: (**a**) reference lubricant (Mistral 15W40) and corresponding nanolubricants, and (**b**) reference biolubricant (PLANTO MOT SAE 10W40) and corresponding nanobiolubricants.

3.4. UV-Vis Analysis of Nanoparticle Dispersion

The stability of the formulated nanolubricants was assessed using a UV-Vis spectrophotometer. This method enabled the determination of peak absorbance and identification of the optimal wavelength from the obtained scan results. The absorbance values

for SiO_2/Mistral 15W40 and SiO_2/PLANTO MOT SAE 10W40 nanolubricants at weight concentrations of 0.25%, 0.50%, 0.75%, and 1.00% are presented in Figure 8, covering wavelengths from 190 nm to 900 nm, which indicates that the peak absorbance for all the tested nanolubricants consistently occurred at a wavelength of 296 nm. The absorbance values recorded at a wavelength of approximately 300 nm characterize the presence of SiO_2 nanoparticles [21,26]. Figure 9 presents the peak absorbance values of SiO_2/Mistral 15W40 nanolubricants at various concentrations and under different preparation conditions (stirring and sonication times) over a 77-day period. The peak absorbance values were measured immediately after preparation (0 days) and at subsequent time points: 1 day, 3 days, 7 days, 15 days, 30 days, 54 days, and 77 days. For the 0.25% SiO_2 sample, the peak absorbance values at 0 days for different sonication times (0 h, 1 h, 2.5 h) are relatively close: 3.478, 3.508, and 3.366, respectively (these values are dimensionless because they are calculated as the logarithm of the ratio of incident light to transmitted light through a sample). Over time, all samples show a gradual decrease in absorbance, with the highest sonication time (2.5 h) exhibiting slightly better stability. For the 0.50% SiO_2 sample, the initial peak absorbance values are lower than those of the 0.25% sample, but show a similar pattern: 2.919, 2.642, and 2.561. Again, the sample with 2.5 h sonication demonstrates better stability over time. For the 0.75% SiO_2 sample, the initial peak absorbance values are 2.407, 2.405, and 2.345. Similar to the previous concentrations, higher sonication times tend to maintain higher absorbance values over time. For the 1.0% SiO_2 sample, the initial peak absorbance values are 2.209, 2.051, and 1.991. The trend of better stability with increased sonication time is observed here as well. Across all concentrations, there is a general decrease in peak absorbance values over the 77-day period. The rate of decrease is faster in the initial days (up to 15 days) and tends to stabilize somewhat after 30 days. Samples with higher initial sonication times (2.5 h) show a slower rate of decrease, indicating better dispersion stability. Higher concentrations (0.75% and 1.0%) show lower initial peak absorbance values compared to lower concentrations (0.25% and 0.50%). Despite this, higher concentrations also show significant improvements in stability with increased sonication times. Figure 10 shows the peak absorbance values of SiO_2/PLANTO MOT SAE 10W40 nanobiolubricants at various concentrations and under different preparation conditions (stirring and sonication times) over a 77-day period. The peak absorbance values were measured immediately after preparation (0 days) and at several subsequent time points: 1 day, 3 days, 7 days, 15 days, 30 days, 54 days, and 77 days. For the 0.25% SiO_2 sample, the initial peak absorbance values are quite close for different sonication times: 3.480, 3.509, and 3.486. Over time, the sample with the highest sonication time (2.5 h) shows a slower rate of decrease, indicating better stability. For the 0.50% SiO_2 sample, the initial peak values are 3.419, 2.967, and 2.678. Samples with 1 h and 2.5 h of sonication show better stability over time, with 2.5-h samples showing the best long-term stability. For the 0.75% SiO_2 sample, the initial values are 2.631, 2.546, and 2.402. Higher sonication times (2.5 h) maintain higher absorbance values for longer periods. For the 1.0% SiO_2 sample, the initial values are 2.426, 2.316, and 2.193. Again, the trend of better stability with increased sonication time is observed. Across all concentrations, peak absorbance values decrease over the 77-day period. The decrease is more pronounced in the initial days (up to 15 days) and tends to stabilize somewhat after 30 days. Samples with longer sonication times (2.5 h) generally show better stability, retaining higher absorbance values over time. Lower concentrations (0.25% and 0.50%) have higher initial absorbance values compared to higher concentrations (0.75% and 1.00%). Higher concentrations benefit more from longer sonication times, showing slower decreases in absorbance.

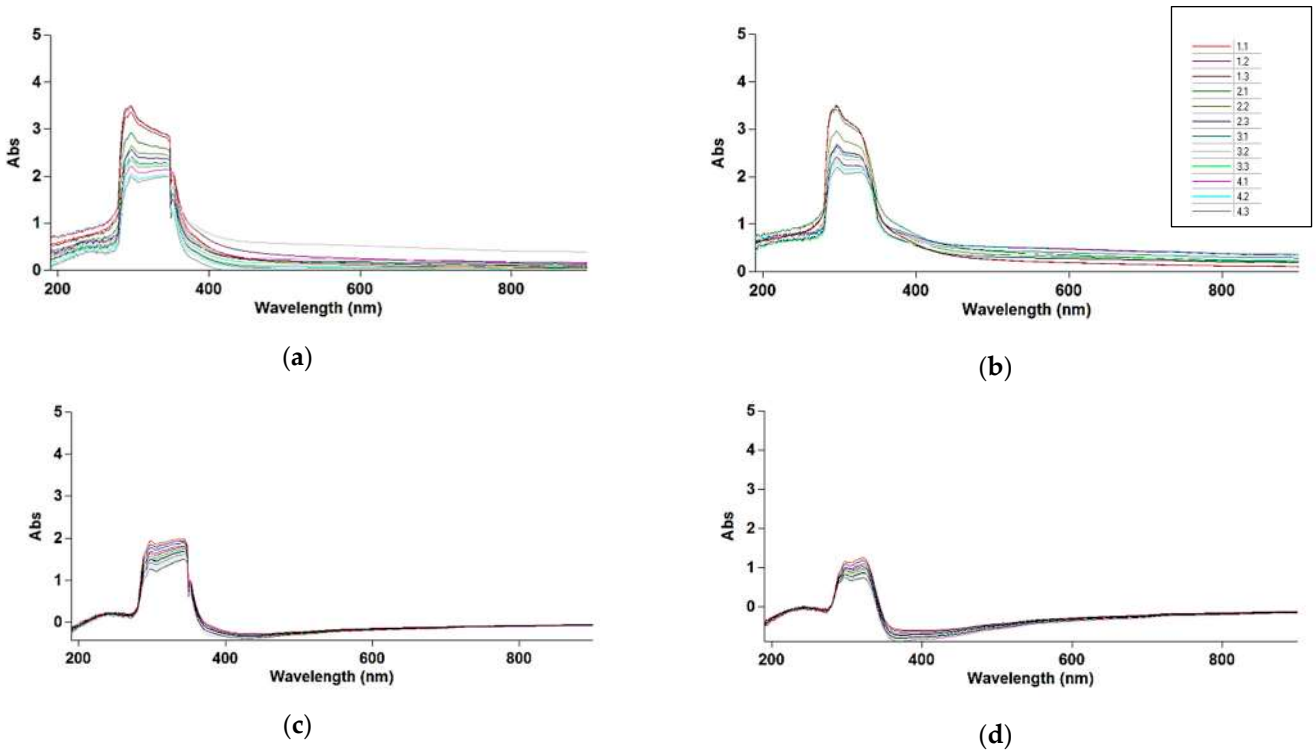

Figure 8. UV-Vis Absorbance of nanolubricants at different weight concentrations of nanoparticles and various sonication times: (**a**) SiO_2/Mistral 15W40 nanolubricants after preparation; (**b**) SiO_2/PLANTO MOT SAE 10W40 nanobiolubricants after preparation; (**c**) SiO_2/Mistral 15W40 nanolubricants after 77 days; (**d**) SiO_2/PLANTO MOT SAE 10W40 nanobiolubricants after 77 days.

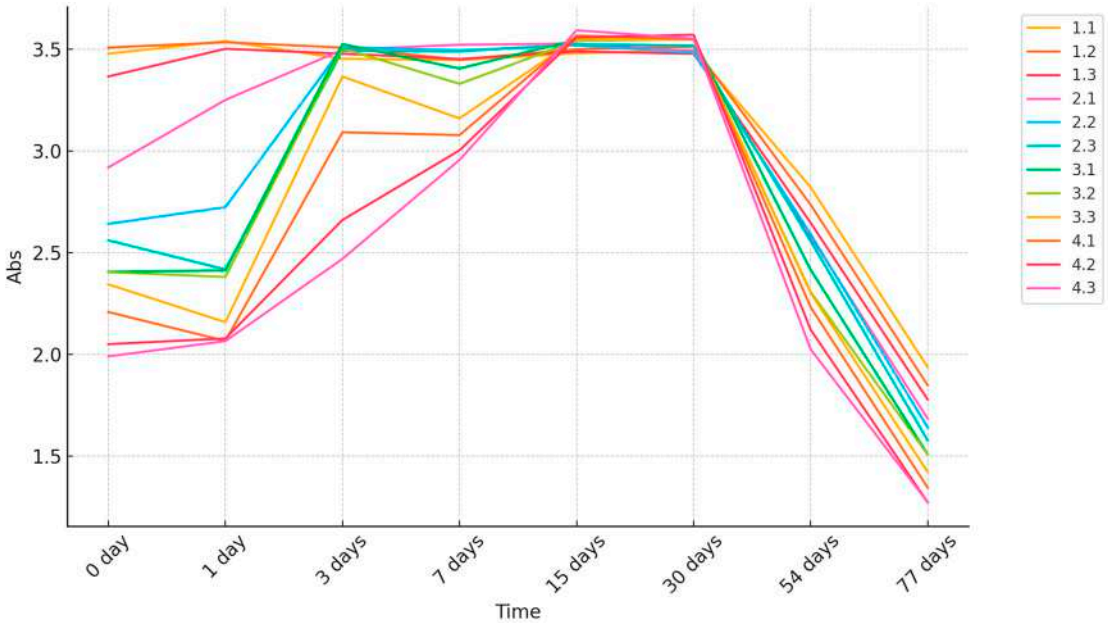

Figure 9. UV-Vis evaluation of SiO_2/Mistral 15W40 nanolubricants for 77 days at different concentrations with different sonication times.

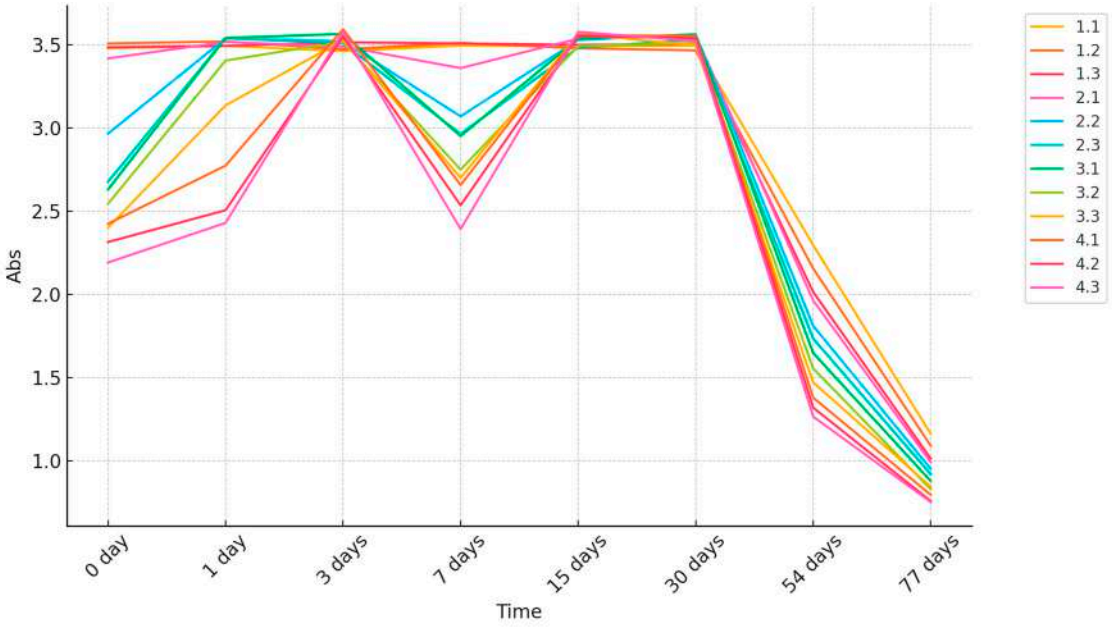

Figure 10. UV-Vis evaluation of SiO_2/PLANTO MOT SAE 10W40 nanobiolubricants for 77 days at different concentrations with different sonication times.

The numerical indices displayed in Figures 9 and 10 refer to Table 4. Each index represents specific combinations of nanoparticle concentration percentages and sonication times.

4. Conclusions

The study demonstrates that incorporating SiO_2 nanoparticles, modified with the silane coupling agent KH570, significantly enhances the physicochemical properties of both conventional and biolubricants. The surface modification facilitates better dispersion of SiO_2 nanoparticles, leading to a stable suspension in the form of clusters. The enhanced lubricants show slight increases in density and viscosity, along with a higher viscosity index, indicating improved thermal stability and flow resistance. These improvements can potentially lead to better lubrication performance, reduced friction, and wear, making the modified lubricants more suitable for demanding industrial and automotive applications. Chemical analysis, including TAN and TBN measurements, confirms that the addition of SiO_2 nanoparticles at various concentrations (0.25%, 0.50%, 0.75%, and 1.00%) does not introduce critical acidity levels and maintains a strong alkaline reserve. Furthermore, the ICP-OES analysis shows that the incorporation of SiO_2 nanoparticles mainly affects the silicon concentration, with minimal impact on other essential additives. This supports the feasibility of using SiO_2 nanoparticles without compromising additive stability. FTIR analysis confirmed the presence of SiO_2 and KH570 without altering the basic functional structures of the lubricants and biolubricants, indicating excellent chemical stability.

The long-term stability of the nanolubricants was evaluated over a period of 77 days. Initial observations indicated well-dispersed samples, with visible sedimentation beginning around the 30th day and becoming more pronounced by the 54th and 77th days. The bio-lubricants exhibited slightly higher sedimentation compared to conventional lubricants. Sonication time influenced stability, with longer sonication times (2.5 h) yielding better stability across different concentrations. UV-Vis spectrophotometry further emphasized the importance of optimizing sonication time to enhance the stability of the nanolubricants, with longer sonication times being beneficial, especially at higher nanoparticle concentrations.

Future research could concentrate on additional domains to enhance and investigate the application of SiO_2 nanoparticles in lubricants. In particular, long-term performance testing in a range of industrial and automotive applications would be beneficial in determining the practical application of lubricants enriched with SiO_2 nanoparticles in real-world

scenarios. To ensure their sustainable use, it would also be crucial to assess the safety and environmental impact of SiO_2 nanoparticle-enhanced lubricants, including how they should be disposed of and any potential effects on ecosystems.

In summary, the addition of surface-modified SiO_2 nanoparticles to conventional and biolubricants enhances their physicochemical properties and stability without compromising chemical stability or additive integrity. The study highlights the importance of optimizing preparation conditions, particularly sonication time, to maximize the benefits of nanolubricants in various applications.

Author Contributions: Conceptualization, H.P., M.R. and M.B.; methodology, H.P.; formal analysis, H.P., M.R. and M.B.; investigation, H.P.; data curation, H.P.; writing—original draft preparation, H.P.; writing—review and editing, H.P., M.R. and M.B.; visualization, H.P.; supervision, M.R. and M.B. All authors have read and agreed to the published version of the manuscript.

Funding: This research received no external funding.

Data Availability Statement: The raw data supporting the conclusions of this article will be made available by the authors on request.

Acknowledgments: The authors wish to thank: Dott. Ivo Cordioli for his useful suggestions about lubricants, and the company management of NILS S.p.A. (Postal, Bolzano, Italy), for letting Homeyra Piri be hosted for an 8-month internship period, thus allowing her to develop a proper expertise about lubricants. The authors wish also to thank NILS S.p.A and FUCHS LUBRICANTS GERMANY GmbH for having provided the lubricant and biolubricant used in the tests free of charge.

Conflicts of Interest: The authors declare no conflicts of interest.

References

1. Luo, J.; Zhou, X. Superlubricitive engineering—future industry nearly getting rid of wear and frictional energy consumption. *Friction* **2020**, *8*, 643–665. [CrossRef]
2. Wang, Y.; Li, D.; Nie, C.; Gong, P.; Yang, J.; Hu, Z.; Li, B.; Ma, M. Research progress on the wear resistance of key components in agricultural machinery. *Materials* **2023**, *16*, 7646. [CrossRef]
3. Joshi, U.; Pandey, K.K.; Uttarakhand, S.G. Lubrication: Purpose, properties, and use in agri-mechanics. *Agric. Food E Newsl.* **2020**, *2*, 622–625.
4. Calcante, A.; Brambilla, M.; Bisaglia, C.; Oberti, R. Estimating the total lubricant oil consumption rate in agricultural tractors. *Trans. ASABE* **2019**, *62*, 197–204. [CrossRef]
5. Asonja, A.; Mikic, D.; Stojanovic, B.; Gligoric, R.; Savin, L.; Tomic, M. Examination of motor oils in exploitation of agricultural tractors in process of basic treatment of plot. *J. Balk. Tribol. Assoc.* **2013**, *19*, 314–322.
6. Bietresato, M.; Calcante, A.; Mazzetto, F. A neural network approach for indirectly estimating farm tractors engine performances. *Fuel* **2015**, *143*, 144–154. [CrossRef]
7. Agricultural Machinery Registrations. Available online: https://www.federunacoma.it/en/statistiche/agricultural-machinery-registrations.php (accessed on 4 March 2024).
8. Zhao, J.; Huang, Y.; He, Y.; Shi, Y. Nanolubricant additives: A review. *Friction* **2021**, *9*, 891–917. [CrossRef]
9. Zilabi, S.; Shareei, M.; Bozorgian, A.; Ahmadpour, A.; Ebrahimi, E. A review on nanoparticle application as an additive. *Adv. J. Chem. Sect. B* **2022**, *4*, 209–221. [CrossRef]
10. Duan, H.; Li, W.; Kumara, C.; Jin, Y.; Meyer, H.M.; Luo, H.; Qu, J. Ionic liquids as oil additives for lubricating oxygen-diffusion case-hardened titanium. *Tribol. Int.* **2019**, *136*, 342–348. [CrossRef]
11. Uflyand, I.E.; Zhinzhilo, V.A.; Burlakova, V.E. Metal-containing nanomaterials as lubricant additives: State-of-the-art and future development. *Friction* **2019**, *7*, 93–116. [CrossRef]
12. Ahmadpour, A.; Bozorgian, A.; Eslamimanesh, A.; Mohammadi, A.H. Photocatalytic treatment of spontaneous petrochemical effluents by TiO_2 CTAB synthetic nanoparticles. *Desalination Water Treat.* **2022**, *249*, 297–308. [CrossRef]
13. Han, K.; Zhang, Y.; Song, N.; Yu, L.; Zhang, P.; Zhang, Z.; Qian, L.; Zhang, S. The Current situation and future direction of nanoparticles lubricant additives in China. *Lubricants* **2022**, *10*, 312. [CrossRef]
14. Chen, Y.; Renner, P.; Liang, H. Dispersion of nanoparticles in lubricating oil: A critical review. *Lubricants* **2019**, *7*, 7. [CrossRef]
15. Chinas-Castillo, F.; Spikes, H.A. Mechanism of action of colloidal solid dispersions. *J. Tribol.* **2003**, *125*, 552–557. [CrossRef]
16. Azman, N.F.; Samion, S. Dispersion stability and lubrication mechanism of nanolubricants: A review. *Int. J. Precis. Eng. Manuf. Green Technol.* **2019**, *6*, 393–414. [CrossRef]
17. Seymour, B.T.; Wright, R.A.; Parrott, A.C.; Gao, H.; Martini, A.; Qu, J.; Dai, S.; Zhao, B. Poly(alkyl methacrylate) brush-grafted silica nanoparticles as oil lubricant additives: Effects of alkyl pendant groups on oil dispersibility, stability, and lubrication property. *ACS Appl. Mater. Interfaces* **2017**, *9*, 25038–25048. [CrossRef] [PubMed]

18. Sui, T.; Song, B.; Zhang, F.; Yang, Q. Effect of particle size and ligand on the tribological properties of amino functionalized hairy silica nanoparticles as an additive to polyalphaolefin. *J. Nanomater.* **2015**, *2015*, 492401. [CrossRef]
19. Sui, T.; Song, B.; Zhang, F.; Yang, Q. Effects of functional groups on the tribological properties of hairy silica nanoparticles as an additive to polyalphaolefin. *RSC Adv.* **2015**, *6*, 393–402. [CrossRef]
20. Gulzar, M.; Masjuki, H.H.; Kalam, M.A.; Varman, M.; Zulkifli NW, M.; Mufti, R.A.; Zahid, R.; Yunus, R. Dispersion stability and tribological characteristics of TiO_2/SiO_2 nanocomposite-enriched biobased lubricant. *Tribol. Trans.* **2017**, *60*, 670–680. [CrossRef]
21. Sharif, M.Z.; Azmi, W.H.; Redhwan, A.A.M.; Zawawi, N.M.M. Preparation and stability of silicone dioxide dispersed in polyalkylene glycol based nanolubricants. *MATEC Web Conf.* **2017**, *90*, 01049. [CrossRef]
22. Eiser, E. Dynamic Light Scattering. In *Multi Length-Scale Characterisation*; Wiley: Hoboken, NJ, USA, 2014; pp. 233–282. [CrossRef]
23. Lin, J.; Wang, L.; Chen, G. Modification of graphene platelets and their tribological properties as a lubricant additive. *Tribol. Lett.* **2011**, *41*, 209–215. [CrossRef]
24. Koshy, C.P.; Rajendrakumar, P.K.; Thottackkad, M.V. Analysis of tribological and thermo-physical properties of surfactant-modified vegetable oil-based CuO nano-lubricants at elevated temperatures-An experimental study. *Tribol. Online* **2015**, *10*, 344–353. [CrossRef]
25. Ramachandran, K.; Navaneethakrishnan, P.; Sivaraja, M. The influence of nickel oxide nanoparticle dispersion on the thermo stability of lubricant oil. *Int. J. Nanosci.* **2020**, *19*, 1850044. [CrossRef]
26. Ismail, M.F.; Azmi, W.H.; Mamat, R.; Sharma, K.V.; Zawawi, N.N.M. Stability Assessment of Polyvinyl-Ether-Based TiO_2, SiO_2, and Their Hybrid Nanolubricants. *Lubricants* **2023**, *11*, 23. [CrossRef]
27. Kashefi, M.H.; Saedodin, S.; Rostamian, S.H. Effect of silica nano-additive on flash point, pour point, rheological and tribological properties of lubricating engine oil: An experimental study. *J. Therm. Anal. Calorim.* **2022**, *147*, 4073–4086. [CrossRef]
28. Cortes, V.; Sanchez, K.; Gonzalez, R.; Alcoutlabi, M.; Ortega, J.A. The performance of SiO_2 and TiO_2 nanoparticles as lubricant additives in sunflower oil. *Lubricants* **2020**, *8*, 10. [CrossRef]
29. Pochi, D.; Fanigliulo, R.; Bisaglia, C.; Cutini, M.; Grilli, R.; Betto, M.; Fornaciari, L. Vegetable-based oil as UTTO fluid for agricultural tractors application. *Appl. Eng. Agric.* **2020**, *36*, 79–88. [CrossRef]
30. Pochi, D.; Fanigliulo, R.; Bisaglia, C.; Cutini, M.; Grilli, R.; Fornaciari, L.; Betto, M.; Pari, L.; Gallucci, F.; Capuzzi, L.; et al. Test rig and method for comparative evaluation of conventional and bio-based hydraulic fluids and lubricants for agricultural transmissions. *Sustainability* **2020**, *12*, 8564. [CrossRef]
31. Rudnick, L.R. (Ed.) *Synthetics, Mineral Oils, and Bio-Based Lubricants: Chemistry and Technology*; CRC Press: Boca Raton, FL, USA, 2020; ISBN 9781351655743. Available online: https://www.routledge.com/Synthetics-Mineral-Oils-and-Bio-Based-Lubricants-Chemistry-and-Technology/Rudnick/p/book/9781138068216 (accessed on 29 June 2024).
32. Malvindi, M.A.; Brunetti, V.; Vecchio, G.; Galeone, A.; Cingolani, R.; Pompa, P.P. SiO_2 nanoparticles biocompatibility and their potential for gene delivery and silencing. *Nanoscale* **2012**, *4*, 486–495. [CrossRef]
33. Tian, S.; Gao, W.; Liu, Y.; Kang, W.; Yang, H. Effects of surface modification Nano-SiO_2 and its combination with surfactant on interfacial tension and emulsion stability. *Colloids Surf. A Physicochem. Eng. Asp.* **2020**, *595*, 124682. [CrossRef]
34. Uzay, Ç. Investigation of physical, mechanical, and thermal properties of glass fiber reinforced polymer composites strengthened with KH550 and KH570 silane-coated silicon dioxide nanoparticles. *J. Compos. Mater.* **2022**, *56*, 2995–3011. [CrossRef]
35. *ASTM D445-24*; Standard Test Method for Kinematic Viscosity of Transparent and Opaque Liquids (and Calculation of Dynamic Viscosity). ASTM: West Conshohocken, PA, USA, 2024. [CrossRef]
36. *ISO 2909:2002*; Petroleum Products–Calculation of Viscosity Index from Kinematic Viscosity. International Organization for Standardization: Geneva, Switzerland, 2002.
37. *ASTM D4052-22*; Standard Test Method for Density, Relative Density, and API Gravity of Liquids by Digital Density Meter. ASTM: West Conshohocken, PA, USA, 2022. [CrossRef]
38. *ASTM D4739-17*; Standard Test Method for Base Number Determination by Potentiometric Hydrochloric Acid Titration. ASTM: West Conshohocken, PA, USA, 2017.
39. *ASTM D664-18e2*; Standard Test Method for Acid Number of Petroleum Products by Potentiometric Titration. ASTM: West Conshohocken, PA, USA, 2018. [CrossRef]
40. Ali, M.K.A.; Hou, X.; Abdelkareem, M.A.A. Anti-wear properties evaluation of frictional sliding interfaces in automobile engines lubricated by copper/graphene nanolubricants. *Friction* **2020**, *8*, 905–916. [CrossRef]
41. Fitch, B.; Noria Corporation. The Critical Role of Viscosity Index in Lubrication. Available online: https://www.machinerylubrication.com/Read/32590/the-critical-role-of-viscosity-index-in-lubrication (accessed on 1 July 2024).
42. Piri, H.; Renzi, M.; Bietresato, M. Technical implications of the use of biofuels in agricultural and industrial compression-ignition engines with a special focus on the interactions with (bio)lubricants. *Energies* **2023**, *17*, 129. [CrossRef]
43. Yu, W.; Xie, H. A review on nanofluids: Preparation, stability mechanisms, and applications. *J. Nanomater.* **2012**, *2012*, 435873. [CrossRef]
44. Azman, S.S.N.; Zulkifli, N.W.M.; Masjuki, H.; Gulzar, M.; Zahid, R. Study of tribological properties of lubricating oil blend added with graphene nanoplatelets. *J. Mater. Res.* **2016**, *31*, 1932–1938. [CrossRef]
45. Amiruddin, H.; Abdollah, M.F.B.; Idris, A.M.; Abdullah, M.I.H.C.; Tamaldin, N. Stability of nano-oil by pH control in stationary conditions. In Proceedings of the Mechanical Engineering Research Day 2015, Melaka, Malaysia, 31 March 2015; pp. 55–56. Available online: https://eprints.utem.edu.my/id/eprint/14424/1/p55_56.pdf (accessed on 7 July 2024).

46. Ali, M.K.A.; Xianjun, H. Role of bis(2-ethylhexyl) phosphate and Al_2O_3/TiO_2 hybrid nanomaterials in improving the dispersion stability of nanolubricants. *Tribol. Int.* **2021**, *155*, 106767. [CrossRef]
47. Ghadimi, A.; Saidur, R.; Metselaar, H.S.C. A review of nanofluid stability properties and characterization in stationary conditions. *Int. J. Heat Mass Transf.* **2011**, *54*, 4051–4068. [CrossRef]
48. Lee, K.; Hwang, Y.; Cheong, S.; Kwon, L.; Kim, S.; Lee, J. Performance evaluation of nano-lubricants of fullerene nanoparticles in refrigeration mineral oil. *Curr. Appl. Phys.* **2009**, *9*, e128–e131. [CrossRef]
49. Jiang, H.; Hou, X.; Dearn, K.D.; Su, D.; Ali, M.K.A. Thermal stability enhancement mechanism of engine oil using hybrid MoS_2/h-BN nano-additives with ionic liquid modification. *Adv. Powder Technol.* **2021**, *32*, 4658–4669. [CrossRef]
50. Kotia, A.; Haldar, A.; Kumar, R.; Deval, P.; Ghosh, S.K. Effect of copper oxide nanoparticles on thermophysical properties of hydraulic oil-based nanolubricants. *J. Braz. Soc. Mech. Sci. Eng.* **2017**, *39*, 259–266. [CrossRef]
51. Haldar, A.; Kotia, A.; Kumar, N.; Ghosh, S.K. Enhancing the tribological properties of hydraulic oil-based nanolubricants using MWCNT-SiO_2 hybrid nanoparticles. *J. Braz. Soc. Mech. Sci. Eng.* **2022**, *44*, 223. [CrossRef]
52. Yadav, L.; Sihmar, A.; Kumar, S.; Dhaiya, H.; Vishwakarma, R. Review of nano-based smart coatings for corrosion mitigation: Mechanisms, performance, and future prospects. *Environ. Sci. Pollut. Res.* **2024**, *31*, 1–27. [CrossRef] [PubMed]
53. Farag, A.A. Applications of nanomaterials in corrosion protection coatings and inhibitors. *Corros. Rev.* **2020**, *38*, 67–86. [CrossRef]
54. Ifeanyi-Nze, F.O.; Akhiehiero, E.T. Optimization of the process variables on biodegradable industrial lubricant basestock synthesis from Jatropha curcas seed oil via response surface methodology. *Front. Energy Res.* **2023**, *11*, 1169565. [CrossRef]
55. Nguyen, H.K.D.; Van Vo, H.; Dinh, N.T. Role of silica on stability of mesoporous rice husk based catalyst and its activity in synthesis of biolubricant stock. *J. Porous Mater.* **2020**, *27*, 1349–1361. [CrossRef]
56. Kamarudin, N.S.B.; Veny, H.; Sidek, N.F.B.; Abnisa, F.; Sazali, R.A.; Aziz, N. Investigation on synthesis of trimethylolpropane (TMP) ester from non-edible oil. *Bull. Chem. React. Eng. Catal.* **2020**, *15*, 808–817. [CrossRef]
57. Song, X.; Fang, C.; Li, Y.; Wang, P.; Zhang, Y.; Xu, Y. Characterization of mechanical properties of jute/PLA composites containing nano SiO_2 modified by coupling agents. *Cellulose* **2022**, *29*, 835–848. [CrossRef]
58. Li, H.; Cheng, B.; Gao, W.; Feng, C.; Huang, C.; Liu, Y.; Lu, P.; Zhao, H. *Recent Research Progress and Advanced Applications of Silica/Polymer Nanocomposites*; De Gruyter Open Ltd.: Warsaw, Poland, 2022; Volume 11, pp. 2928–2964. [CrossRef]